Circulation Over the Continental Shelf of the Southeastern Bering Sea

5

Thomas H. Kinder[1] and James D. Schumacher[2]

National Space Technology Laboratories Station,

[1] Naval Ocean Research and Development Activity,
Bay St. Louis, Mississippi

[2] Pacific Marine Environmental Laboratory,
Environmental Research Laboratories/National
Oceanic and Atmospheric Administration
Seattle, Washington

ABSTRACT

Using extensive direct current measurements made during the period 1975-78, we describe flow over the southeastern Bering Sea shelf. Characteristics of the flow permit us to define three distinct regimes, nearly coincident with the hydrographic domains defined in the previous chapter. The coastal regime, inshore of the 50 m isobath, had a slow (1-5 cm/sec) counterclockwise mean current and occasional wind-driven pulses of a few days' duration. The middle regime, bounded by the 50 and 100 m isobaths, had insignificant (<1 cm/sec) mean flow but relatively stronger wind-driven pulses. The outer regime, between the 100 m isobath and shelf break (~170 m), had a 1-5 cm/sec westward mean and low-frequency events unrelated to local winds. Over the entire shelf most of the horizontal kinetic energy was tidal, varying from 60 percent in the outer regime to 90 percent in the coastal regime. About 80 percent of the tidal energy was semidiurnal.

Mean flow over the shelf is well described qualitatively by dynamic topographies, and shallow current data from both coastal and outer regimes agree quantitatively as well. Two meteorological conditions that force the observed current pulses have been identified. In summer eastward-traveling low atmospheric pressure centers caused low-frequency pulses in the middle regime, and weaker pulses in the coastal regime. In winter, outbreaks of cold and dry continental air forced pulses within the coastal and middle regimes.

INTRODUCTION

Until recently, few direct current measurements were available over this shelf, so that ideas about flow were based partly on indirect methods and partly on intuition (see the historical review which follows). Since 1975, however, we and many colleagues have gathered numerous direct current measurements with concurrent hydrographic data. We are thus able to base our characterization of the flow over this shelf on plentiful information. Our analysis of this suite of data (Table 5-1) is still incomplete. We expect further analysis building on this preliminary report to improve understanding, but not to change fundamentally the conclusions that we present here.

The most important discovery as a result of these new data is the existence of three distinguishable flow regimes over the shelf. These flow regimes correspond closely to the hydrographic domains outlined in the preceding chapter. The coastal regime is shoreward of the 50 m isobath, the middle regime is between the 50 m and 100 m isobaths, and the outer regime is between the 100 m isobath and the shelf break. Seaward of the shelf break lies the oceanic regime. Although they nearly coincide, for clarity we refer to flow *regimes* and hydrographic *domains* in this and the previous chapter.

We emphasize the characteristics of these regimes as we examine the frequency distribution of the horizontal kinetic energy, the mean circulation, and seasonal variations. Before discussing our findings, we review the physical setting, highlight earlier work, and discuss our measurements.

Setting

The southeastern shelf is bounded by the Alaska Peninsula, the Alaskan mainland, the shelf break

running from Unimak Pass to the Pribilof Islands, and an arbitrary line running from the Pribilofs to Nunivak Island (Fig. 5-1). The shelf break occurs at an average depth of 170 m (Scholl et al. 1968), and the shelf shoals gradually over a featureless expanse of 500 km. Flow over the continental slope is highly variable (Kinder et al. 1975, Coachman and Charnell 1979, Kinder et al. 1980) with mean flow to the northwest at 5-10 cm/sec. The shelf regime is separated from the adjacent oceanic regime by a weak haline front (Kinder and Coachman 1978, Coachman and Charnell 1979). We have found no convincing evidence for exchange of mass or momentum between the shelf and oceanic regimes by eddies or rings. This characteristic is probably the effect of some combination of the width of the shelf, the front overlying the slope, and the weakness of the boundary current above the slope. At the same time, a considerable volume of water must flow across this long (~1,000 km) shelf break somewhere: about 1×10^6 m^3/sec flows northward through the Bering Strait into the Chukchi Sea (Coachman and Aagaard,

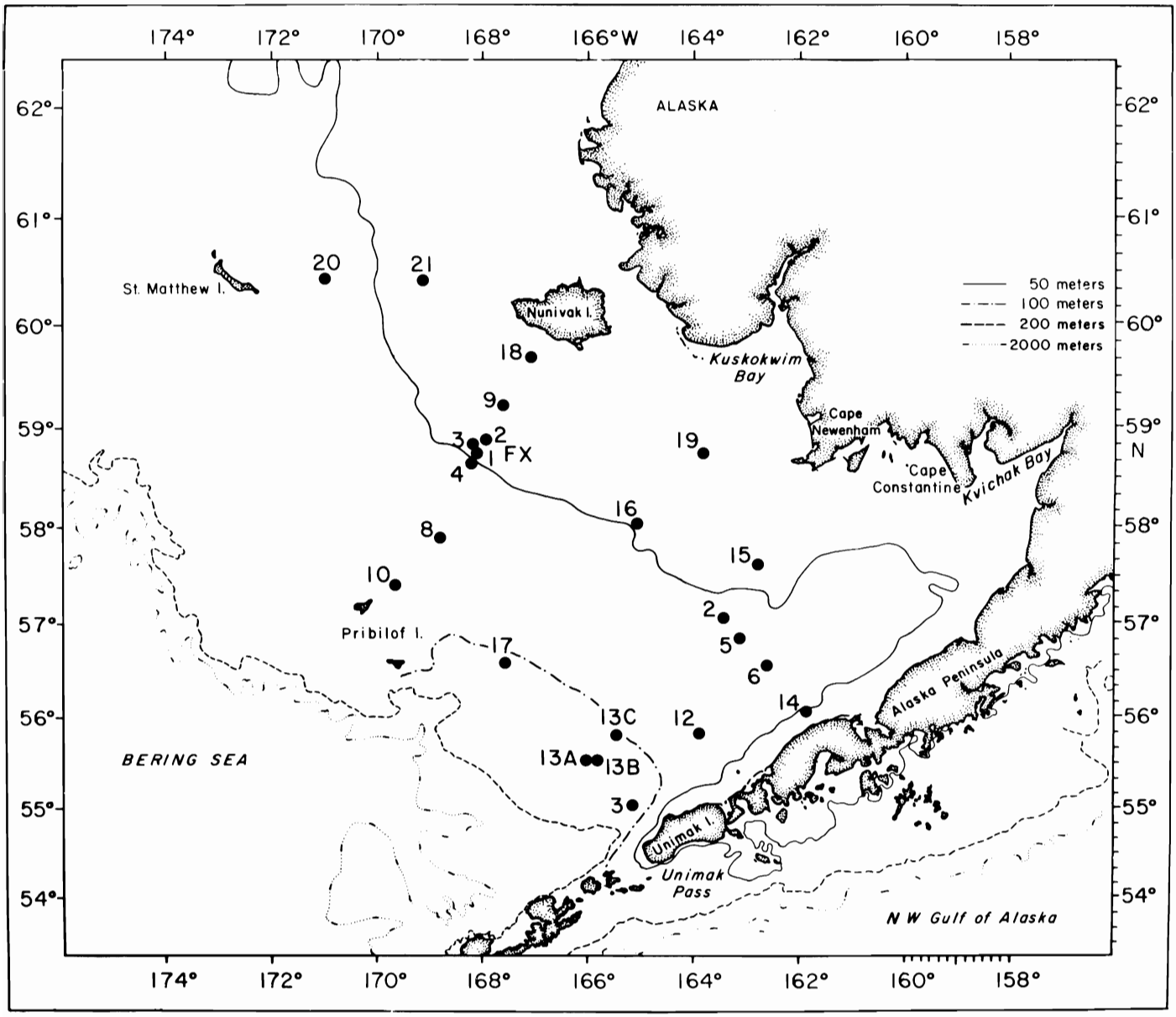

Figure 5-1. Locations of current-meter moorings. Most moorings had two current meters, one 10 m above bottom and one 20 m below the surface. BC signifies Bristol Bay project and FX signifies Frontal Experiment. Sequential deployments at a mooring site are designated by letter suffixes, e.g., BC-9A. The three moorings southwest of Nunivak Island numbered 1-3 have FX prefixes; all others have BC prefixes.

Chapter 8, this volume) and river runoff and precipitation account for only about 2 percent of this. There is strong evidence that little of this required flow occurs southeast of the Pribilofs, and hydrographic distributions suggest that it occurs near Cape Navarin on the Siberian coast.

As we have explained more fully in the previous chapter, the shelf has three distinct hydrographic domains delimited by the 50 m and 100 m isobaths and by the shelf break (170 m isobath). Freshwater runoff from rivers at the coast and an excess of precipitation over evaporation maintain a surface salinity difference across the shelf of about 2°/oo. First-year ice covers most of the shelf during winter, and the weather also changes with the season: these changes are discussed more fully in the chapters on ice (Pease, McNutt, this volume) and on weather (Overland, Niebauer, and Ingraham, this volume).

In summary, five factors influence shelf circulation:

(1) The width of the shelf and the weak haline front over the slope separate much of the shelf from the adjacent oceanic water masses.
(2) There is no strong boundary current adjacent to the shelf.
(3) The shelf has three distinct hydrographic domains.
(4) River runoff maintains a salinity gradient across the shelf.
(5) Weather and ice cover vary annually.

HISTORICAL REVIEW

Until recently, investigators faced the serious problem that there were few data from which inferences about circulation could be made. And yet the need existed for those conducting such non-physical studies as geological, biological, and fisheries studies to know the circulation. For this reason circulation schemes were proposed based on various mixtures of current measurements, hydrographic measurements, drifter measurements, and large doses of intuition. It is not surprising that many of these inferences do not compare favorably with our present knowledge, but some ideas resulting from these early attempts do agree with our present ideas. There are long reference lists of earlier work in Arsenev (1967), Ohtani (1973), and Favorite et al. (1976).

Before 1975 direct current measurements virtually did not exist. A single 24-hour current measurement taken close to Nunivak Island during August 1934 indicated northward flow at 17 cm/sec (Barnes and Thompson 1938). During the summers of 1955 and 1956 the *Tokei Maru* attempted current measurements north of the Alaska Peninsula, but mean currents were obscured by the tides (International North Pacific Fisheries Commission 1957). Hebard (1961) reported June 1957 current measurements at four sites. Each measurement lasted 39 hours, and he inferred a cyclonic (counterclockwise) mean flow around Bristol Bay. Kinder and Coachman (1975) placed three current-meter moorings in Pribilof Canyon for two weeks during July 1974. They measured vector mean speeds from 0.6 to 10.8 cm/sec, and directions mostly parallel to the local isobaths. Some efforts were also made to infer currents from drift bottle experiments (e.g., Thompson and Van Cleve 1936, Dodimead et al. 1963), but little was learned from the few recoveries.

Attempts were also made to describe the circulation using dynamic topographies. On the face of it these attempts seem forlorn, for neglected forces (e.g., friction, sea surface slope, wind stress) may be more important than those retained (i.e., Coriolis and the pressure gradient caused by varying density). In spite of this, mean flows on shelves are often qualitatively described by dynamic topographies, and some features in the Bering topographies agree with direct measurements. Natarov (1963) showed a surface topography (relative to 1,000 db[1]) with broad northward flow across the shelf for summer 1959. Arsenev (1967) constructed a similar map of summer surface current based on 1,000 db. His map showed about 10 cm/sec cyclonic circulation in Bristol Bay, two eddies farther seaward, and northeastward (i.e., shoreward) flow between the Pribilofs and Nunivak Island. Adding wind-driven (Ekman) current weakened one eddy and changed the Pribilofs-Nunivak flow to northwestward. Neither Natarov nor Arsenev explained their method for extrapolating dynamic topography relative to 1,000 db from the deep basin across the shelf. Ohtani (1973) also calculated a surface dynamic topography, using a reference level of 50 db (his calculations did not extend inshore of the 50 m isobath). He showed a broad northwestward flow, but cautioned that such topography has limited application in shallow water.

Attempts were also made to deduce the flow from examination of hydrographic properties. Kitano (1970) apparently thought that the cold bottom water over the middle shelf in summer was advected southeastward from the Gulf of Anadyr (northwestern Bering Sea shelf). Conversely, Takenouti and Ohtani (1974) showed flow in the opposite direction

[1] One decibar (db) is approximately equivalent to one meter depth.

through the middle shelf based on their perception of shelf water masses.

Finally there were circulation schemes, opinions of various authors based on the meager useful data available and their own intuition. The U.S. Navy Hydrographic Office (1958, reproduced by Hughes et al. 1974 as their Fig. 3.4) reported mean currents of 0.1- 0.5 knots (5-25 cm/sec) across the southeastern shelf based on ship drift; a later publication (Naval Oceanographic Office 1977) revealed that this erroneous result was not based on data (Brower et al. 1977 showed a similar circulation in their Figs. 3 and 4). The most ambitious attempt was by Favorite et al. (1976, their Figs. 41 and 42). They hypothesized mean flow paralleling the shelf break (transverse current, identical to Kinder, Coachman, and Galt's 1975 Bering Slope Current), flow onto the shelf paralleling the Alaska Peninsula (West Alaska Current), cyclonic flow around Bristol Bay, no flow over most of the middle shelf, and a southwestward current from near Kuskokwim Bay toward the Pribilofs (Pribilof Current). They did not assign speeds to these flows, but recent data support their general scheme, except for the Pribilof Current.

In general, early attempts to describe flow over the shelf were unsuccessful and even deceptive. The few direct measurements used were overwhelmed by tidal currents and of too short duration to resolve the mean. Dynamic heights referred to 1,000 db were alleged to show flow over the shelf. Local transformations of water masses were ignored and distributions of temperature and salinity were attributed solely to advection. Circulation schemes were drawn showing more detail than the evidence justified. We present our own circulation scheme of the mean flow later in this chapter but we hope that it is used with two questions in mind: What is the *statistical* significance of this depiction of the mean flow? What is the *physical* significance of the mean flow?

METHODS

Measurements

Our inferences are based on 60 current-meter time-series records made during 1975-78 (Table 5-1, Fig. 5-1). Usable record lengths varied from 9 to 246 days, and a total of about 16 record-years of data were obtained. All data were acquired by RCM-4 Aanderaa current meters on taut-wire moorings. Typical instrument locations were 20 m below the surface and 10 m above bottom, as we avoided both the most active part of the surface layer and the bottom boundary layer. Since we also wanted the shallowest instrument on each mooring to be above the seasonal pycnocline, which averaged about 20 m deep, shallow instrument placement was a compromise. Much has been written about the peculiarities of these instruments, and their possible errors due to "rotor pumping," mooring motion, and rotor stalling (Quadfasel and Schott 1979 give several references). In our measurements these errors were minimized by:

(1) use of subsurface flotation (although the upper float was typically within 20 m of the surface);
(2) short mooring length, all less than 200 m and typically less than 100 m;
(3) use of taut moorings, about 1,000 lb (1 lb = 4.45 newton) buoyancy;
(4) large and persistent (tidal) scalar speeds, preventing rotor stalling;
(5) large tidal currents, which maintained relatively steady vane alignments.

All the data that we use have been averaged in some manner, so that random errors are not a serious problem. Biases will not average out, and we estimate direction accurate to ±5° and speeds within ±1 cm/sec (exclusive of rotor pumping and mooring motion). Mayer et al. (1979) discussed similar moorings, and found an erroneous increase in energy up to two-fold (i.e., 40 percent speed increase) in winter on the middle Atlantic shelf. In the Bering Sea strong summer storms are infrequent, and ice cover severely damps surface waves during much of the winter, so that these estimates seem too high for our moorings.

We estimated the speed error by examining the most energetic tidal constituent, the principal lunar semidiurnal (M_2). From records BC-9B and BC-20B (see Table 5-1 and Fig. 5-1) we took one-month segments from the shallow (23 m and 22 m depth) instruments. We compared periods when the mooring was beneath ice cover to periods when the surface was free of ice, assuming that the ice damps surface waves (e.g., Wadhams 1978) so that there was no error induced by waves during the period of ice cover. We further assumed that the M_2 constituent was unchanged by ice cover (it may be affected, but it is probably diminished by ice, making our calculations conservative; see Chapter 8, Pearson et al., this volume). We found a 19-26 percent speed increase during the ice-free season. Although the errors probably vary significantly with weather, we believe that our speeds are accurate to about 25 percent near 20 m depth, and the speeds from deeper instruments are probably more accurate than this.

We also used drifters, floating buoys with "window shade" drogues at 10 m or 17 m depths. The tracks of these surface buoys closely correspond to the tra-

TABLE 5-1

Current-meter records

Mooring	Water depth (m)	Meter depth (m)	Scalar speed (cm/sec)	Vector mean speed (cm/sec)	Direction (°T)	Record length Days	Period
				COASTAL REGIME			
FX-1A	48	38	21.2	1.7	294	63	7/20-9/20/78
FX-2A	43	20	32.4	1.9	306	63	7/19-9/20/78
FX-3A	46	14	33.1	2.3	319	63	7/20-9/20/78
		36	21.9	1.7	295	63	7/20-9/20/78
BC-9A	41	17	28.0	0.1	248	60	6/2-7/31/76
		27	24.8	0.4	251	60	6/2-7/31/76
BC-9B	41	23	28.6	4.4	309	231	9/24/76-5/12/77
		33	16.1	2.9	311	231	9/24/76-5/12/77
BC-9C	41	23.5	24.6	1.0	316	122	5/12-9/10/77
		33.5	19.3	0.9	279	120	5/12-9/8/77
BC-14A	51	20	34.9	1.4	086	31	5/29-6/28/76
		20	33.1	4.8	065	33	8/27-9/28/76
		37	27.4	2.1	211	31	5/29-6/28/76
		37	20.6	0.6	345	33	8/27-9/28/76
BC-15A	50	20	28.8	2.4	274	118	5/31-9/26/76
BC-15C	50	20	29.9	2.2	273	130	5/4-9/10/77
		34	22.4	1.0	304	130	5/4-9/10/77
BC-16A	49	20	28.2	0.5	314	131	5/3-9/10/77
		37	21.2	0.2	011	131	5/3-9/10/77
BC-18A	31	20.5	24.5	1.2	011	122	5/12-9/12/77
BC-19A	28	22.5	27.6	0.8	156	12	5/12-5/23/77
				MIDDLE REGIME			
BC-2A	65	20	17.2	0.5	306	58	9/8-11/5/75
		50	10.0	0.9	301	59	9/8-11/5/75
BC-2B	65	50	17.6	1.2	089	192	11/5/75-5/14/76
BC-2C	65	20	14.8	0.8	324	119	5/31-9/26/76
BC-2D	65	21	17.1	1.9	080	194	9/27/76-4/8/77
BC-2E	65	20	16.9	0.7	214	130	5/4-9/10/77
		50	15.3	0.3	251	130	5/4-9/10/77
BC-4A	55	30	29.3	2.7	299	58	9/8-11/4/75
		47	21.9	0.6	311	58	9/8-11/4/75
BC-4B	55	30	25.4	2.0	301	209	11/5/75-5/31/76
BC-4C	55	25	27.8	2.7	312	61	6/1/76-7/31/76
		52	19.5	1.3	299	61	6/1/76-7/31/76
BC-4D	55	20	31.9	3.6	310	119	9/25/76-1/21/77
		48	18.2	3.0	313	174	9/25/76-3/17/77
BC-4E	55	20	27.7	1.1	300	64	5/13/77-7/15/77
		48	18.3	0.4	274	45	5/13/77-6/28/77
BC-4G	55	18	30.1	3.9	294	64	7/19-9/20/78
		46	16.9	2.1	302	64	7/19-9/20/78
BC-5A	70	20	19.6	1.2	253	31	5/29-6/28/76
		20	15.5	0.2	350	33	8/27-9/28/76
		50	27.8	0.9	298	31	5/29-6/28/76
		50	31.6	1.8	170	33	8/27-9/28/76
BC-6A	76	20	11.3	0.6	012	123	5/29-9/28/76
		50	23.3	0.7	023	31	5/29-6/28/76
		50	18.2	1.4	059	33	8/27-9/28/76
BC-8A	73	26	21.8	0.9	089	60	6/1-7/31/76
		54	21.9	0.6	348	60	6/1-7/31/76

TABLE 5-1, cont.

Mooring	Water depth	Meter depth	Scalar speed	Vector mean speed	Direction	Record length	Period
BC-10A	66	49	21.9	2.0	171	68	6/1-8/8/76
BC-12A	95	39	9.2	0.6	278	84	3/19-6/11/76
			OUTER REGIME				
BC-3A	115	20	29.0	3.2	011	130	11/7/75-3/16/76
BC-3B	116	25	27.8	2.8	334	9	3/17-3/25/76
		105	17.4	1.2	342	73	3/17-5/28/76
BC-3C	114	20	31.8	17.2	012	123	5/29-9/28/76
		100	20.5	6.7	000	123	5/29-9/28/76
BC-13A	122	20	20.6	3.3	353	69	3/22-5/29/76
		100	11.9	1.6	348	87	3/22-6/16/76
BC-13B	115	100	17.3	1.6	335	36	6/6/76-7/12/76
BC-13C	108	22	25.2	5.3	333	202	9/29/76-4/19/77
		96	16.1	4.4	321	83	9/29-12/21/76
BC-17A	104	96	18.1	3.2	296	142	9/22-3/11/77
			ST. MATTHEW				
BC-20A	64	22	23.8	3.4	335	157	9/17/77-2/20/78
		52	16.7	1.4	356	177	9/17/77-3/13/78
BC-20B	64	51	14.6	2.8	334	54	7/21-9/13/78
BC-21A	42	29	32.4	1.5	292	246	9/16/77-5/20/78
BC-21B	42	20	28.8	2.3	338	55	7/20-9/13/78
		32	20.3	0.8	317	55	7/20-9/13/78

The prefix (i.e., BC, FX) indicates the project (Bristol Bay or Frontal Experiment), and indicates the number of the mooring location. The suffix refers to a particular deployment, and individual instruments are identified by their depths. Thus BC-9B 20 m refers to a record obtained at 20 m depth from the second deployment at mooring 9 by the Bristol Bay Project (Fig. 5-1 shows locations). Some records are separated because of midsummer biological fouling problems encountered near the Alaska Peninsula (e.g., BC-14A).

jectories of water parcels at drogue depths. Using the Nimbus satellite, the position of these drifters was fixed about four times daily. This time series of positions (error = ±4 km) was then processed to yield velocities. Kinder et al. (1980) discuss this technique in more detail.

Processing

Sample intervals of the current meters varied from ten minutes to one hour, depending on the expected length of deployment. All data were filtered, with one or two low-pass filters (i.e., they pass low frequencies and block higher ones). All data were originally filtered with a three-hour filter to minimize high-frequency noise. To examine lower frequencies, a further 35-hour low-pass filter was used to remove the tides. Table 5-2 lists basic filter properties, and Charnell and Krancus (1976) discuss processing details.

The 3-hour low-pass filter removes unwanted (for our purposes) high-frequency data, while the 35-hour filter removes diurnal and semidiurnal signals while leaving periods longer than about two days intact. Note that 50 percent amplitude corresponds to 25 percent kinetic energy; the commonly used "half-power point" occurs at longer periods (lower frequencies) than the 50 percent amplitude point.

TABLE 5-2

Filter properties

	Period (hours) with given % amplitude remaining		
	0.1%	50%	99%
3-Hour Filter	2	2.9	5 hours
35-Hour Filter	25	35	55 hours

FREQUENCY DISTRIBUTION OF HORIZONTAL KINETIC ENERGY

One of the most useful ways of examining time-series data of water velocity is to calculate the kinetic energy distribution as a function of frequency. Some of the ocean's processes occur at distinct frequencies, or in discernible frequency bands: often a chaotic jumble in plots of velocity versus time becomes clear when energy versus frequency is plotted. The most striking example is the tidal currents, whose frequencies are determined by astronomical constants.

For the southeastern shelf, we define three frequency categories: mean, low-frequency (subtidal), and tidal. The mean flow is the vector average over a few months or longer. We have in mind the flow over a season or longer, but in practice we have usually defined the mean by the length of the current record. Two tidal periods stood out, diurnal (about 24-hour period) and semidiurnal (about 12-hour period). Low-frequency (long period) flow then fell between seasonal and daily periods. Although there were no definite periods associated with the low-frequency energy, one week was typical. In most records, these three frequency categories contained over 90 percent of the kinetic energy. Tidal frequencies contained most of the energy over the shelf, ranging from 60 percent of the fluctuating energy[2] near the shelf break to more than 95 percent in some records obtained inshore of the 50 m isobath. Roughly 80 percent of this tidal energy was semidiurnal, and 20 percent diurnal (Pearson et al., Chapter 8, this volume, describe the tides more fully). Vector mean speeds were usually 10 percent or less of the mean scalar speeds (Table 5-1), so that the kinetic energy of the mean flow was about 1 percent of the total horizontal kinetic energy ($KE=MV^2/2$, or per unit mass $KE/M=V^2/2$). Of the 60 records in Table 5-1, only three had vector mean speeds exceeding 5 cm/sec, while only six records had scalar mean speeds below 15 cm/sec. Low-frequency flow, that appearing at frequencies between those of tidal and mean flow, accounted for 3-20 percent of the energy. Over the outer shelf, energies in this frequency band were higher than farther inshore. Frequencies in these bands matched frequencies of weather phenomena, say 2-10 days (see weather chapters), and of the inherent variability of the mean flow over the outer shelf and slope (e.g., eddies and meanders). The inertial period (about 14 hours at 58° latitude), which is important in many open-ocean records of kinetic energy, accounted for only 1 percent or less of the total energy in our records. Table 5-3 illustrates the frequency distribution of the horizontal kinetic energy in some typical records.

[2] The fluctuating kinetic energy (per unit mass) is the total kinetic energy, less the kinetic energy of the mean ($FE=\frac{1}{2}(U-\bar{U})^2$). It is often referred to simply as the energy or total energy and is equal to one-half the variance.

Basic plots

We can illustrate the character of flow over the shelf most clearly by showing plots of typical velocity records. Although there were significant differences between records and between regimes, we attempt to highlight common features of the records.

Fig. 5-2 shows unfiltered data from BC-15A (Fig. 5-1) at a depth of 20 m during September 1976.[3] Samples are plotted every 20 minutes (the current-meter sample interval) as two components. The upper plot is the east-west component (U), with eastward flow positive, and the lower plot is the north-south component (V), with northward flow positive. Two features are obvious from this depiction. First, a tidal signal overwhelmed any other variable signals present, and it was mostly semidiurnal (about 12-hour period). This record came from the coastal regime, where the tides contributed 90 percent of the fluctuating kinetic energy, and where the semidiurnal tide typically accounted for 80 percent of the tidal energy. Second, the upper plot is displaced below the zero axis, while the lower plot is centered about this line. Thus, for the week shown,

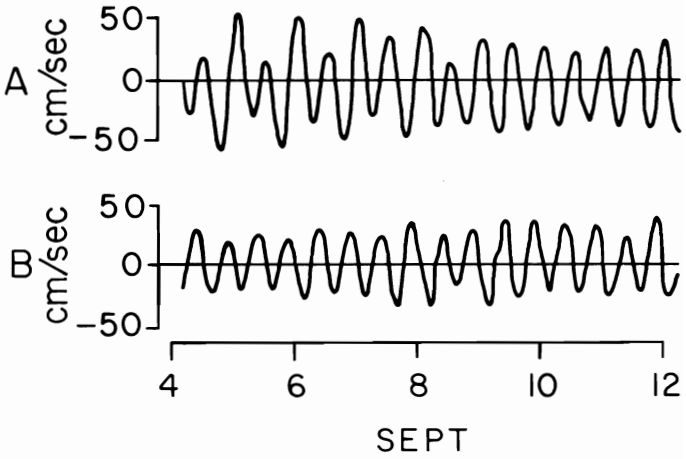

Figure 5-2. A portion of BC-15A 20 m in September 1976. This record is unfiltered, and the sampling interval was 20 minutes. A. East-west (U) velocity component and B. North-south (V) velocity component. Strong semidiurnal and less strong diurnal tides show clearly. The U component is displaced below the axis, indicating a mean flow to the west.

[3] The draftsman has inadvertently low-pass filtered this record somewhat. Original plots made with fine pens show considerably more jiggles (high-frequency energy).

TABLE 5-3

Frequency distribution of horizontal kinetic energy (cm^2/sec^2)[1]

Record	Mean	Fluctuating[2]	Low	Diurnal	Semi-diurnal	Inertial
Coastal Regime						
BC-9B, 23 m, winter	2(0)	434(100)	59(14)	74(17)	271(62)	1(0)
BC-9C, 23 m, summer	1(0)	340(100)	6(2)	73(21)	256(75)	0(0)
Middle Regime						
BC-2B, 50 m, winter	1(0)	203(100)	11(5)	68(33)	120(59)	0(0)
BC-2C, 20 m, summer	0(0)	175(100)	3(2)	49(28)	110(63)	1(1)
Outer Regime						
BC-3C, 100 m, summer	20(8)	266(100)	30(11)	42(16)	165(62)	2(1)
BC-3C, 20 m, summer	148(29)	510(100)	149(29)	60(12)	251(49)	7(1)
BC-3A, 20 m, winter	5(1)	511(100)	112(22)	65(13)	285(56)	6(1)

[1] cm^2/sec^2 is a unit of energy per unit mass, i.e., erg/g (1 erg/g = 10^{-4} J/kg).

[2] Fluctuating kinetic energy is the total kinetic energy in the records, less the kinetic energy of the mean. It is one-half the record variance.

Note that the semidiurnal tidal energy does not change much between summer and winter. Percent of fluctuating energy is shown in parentheses.

the mean current was westward (cf. record mean of 2.4 cm/sec at 274°T). The entire BC-15A record had one of the clearest and most consistent means of all those that we have examined, but usually attempting to measure average currents in flows like this with records of a few days would be futile.

Fig. 5-3 shows a different presentation, progressive vector diagrams (often abbreviated PVD), all smoothed with the three-hour low-pass filter. Progressive vector diagrams show what the trajectory of a water parcel *would* have been *if* it had had the velocity measured at the site of the current meter. This is much different from familiar depictions of flow such as trajectories (paths of particles) or streamlines (lines parallel to velocity vectors). Fig. 5-3 shows progressive vector diagrams from each of the three regions: outer (BC-13A 20 m), middle (BC-6A 50 m), and coastal (BC-15A 20 m). The record mean was largest at the outer mooring (note different distance scales), and least at the middle mooring. All records had vigorous clockwise tidal motion, which was nearly circular in the inner record, and elliptical in the middle record (major axis parallel to the local isobaths). During much of the outer record the tidal circles were superposed on strong low-frequency flow so that they appear as cusps. These subtidal frequency pulses typically lasted for a few days (time may be inferred in Fig. 5-3 by counting clockwise semidiurnal circles), and can be seen in all three records. In the outer record, both speed and direction of pulses were variable. The middle and coastal records showed pulses that appeared similar at each occurrence, northward at BC-6A and westward at BC-15A. Our division of the flow into three frequency bands (mean, low-frequency, tidal) can be seen in each of these examples, and the examples also emphasize the unsteadiness of the flow.

Low-frequency plots

To examine the low-frequency (subtidal) flow, the 35-hour low-pass filter was applied to records before plotting. Plots of components versus time (Fig. 5-4A, 4B) and stick plots (Fig. 5-4C) were then made. Stick plots are a time series of vectors, the base of the

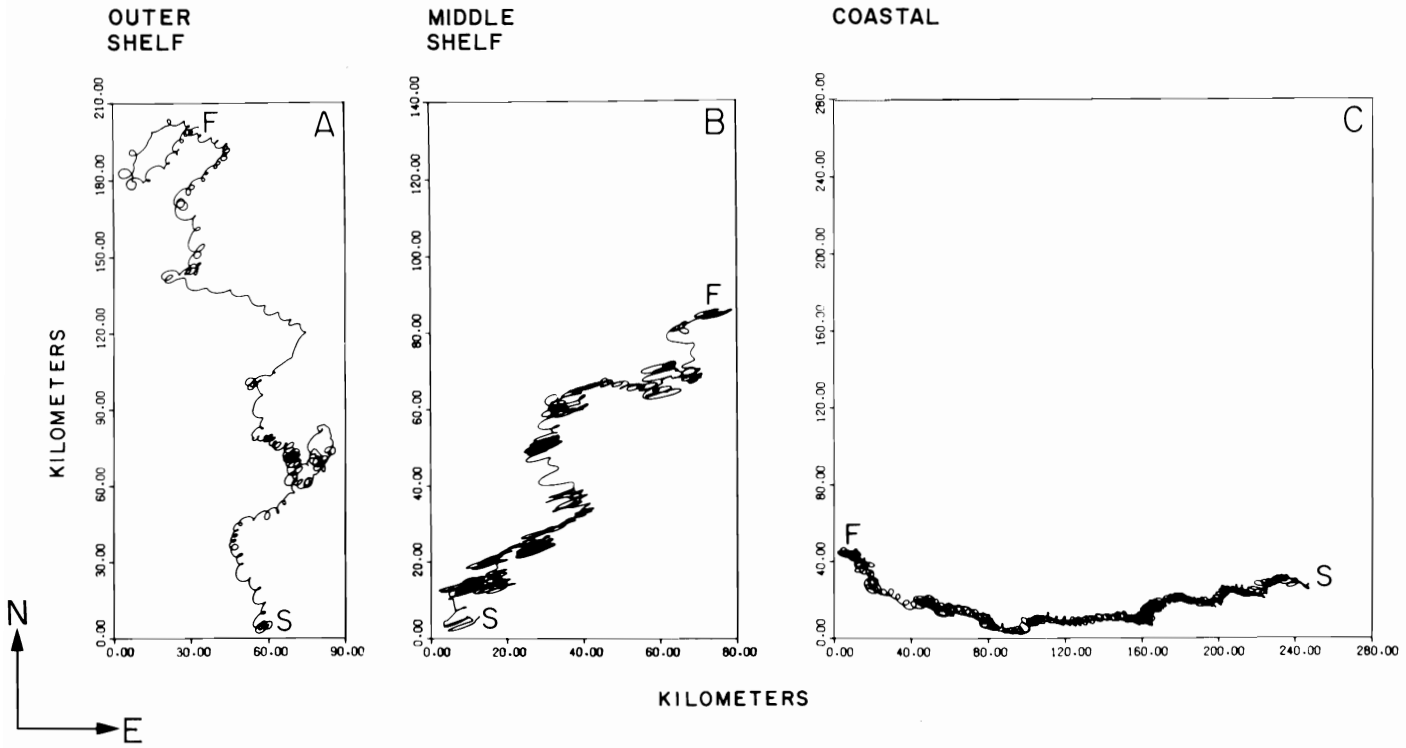

Figure 5-3. Progressive Vector Diagrams (A) Outer regime, BC-13A 20 m. (B) Middle regime, BC-6A 50 m. (C) Coastal regime, BC-15A, 20 m. These figures are the displacement of a water parcel having the same velocity as measured by the current meter, and may be quite different from the actual trajectory of any parcel. The outer record showed tides (cusps), strong pulses, and a northward mean. The middle record showed strong tides (clockwise ellipses), weak northward pulses, and perhaps a weak northeastward mean. The coastal record showed strong tides, westward pulses (extending the tidal circles like a loose spring or slinky toy), and a strong westward mean. Note different scales. (S signifies the start and F the finish of each plot.)

vector indicating the time, the direction away from the base indicating the direction toward flow, and the length of the vector indicating speed. The record from BC-15A at a depth of 20 m shows generally westward flow at 5 cm/sec, with higher speeds later in the record. We found that during the generally low wind speeds (<5 m/sec) in summer there was little correlation between wind and current. During strong winds (>10 m/sec), especially in autumn when higher winds are common and we have many records, wind and currents were much better correlated. The record segments with close correlation seemed to occur for two to four days during the passage of atmospheric low-pressure centers through the area.

Spectra

Except for truly dominant frequency components (e.g., tides), it is difficult to describe the frequency distribution of the records from the plots we have presented thus far. A useful technique for doing this (and the one used to make the estimates for Table 5-3) is spectral analysis. A time series is mathematically (Fourier) transformed, so that instead of velocity as a function of time, we have kinetic energy as a

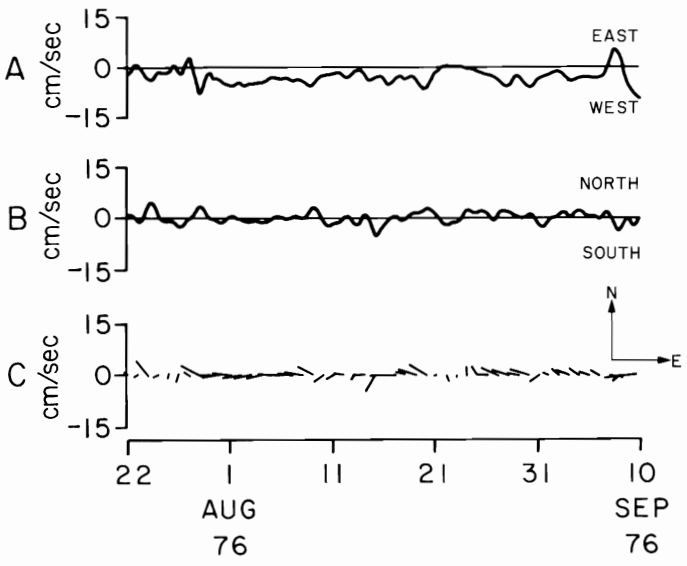

Figure 5-4. Low-frequency flow. Low-pass (35-hour) filtered data from BC-15A 20 m. (A) East-west component, (B) North-south component, and (C) Vector sticks (cm/sec). Much of the low-frequency flow occurred during strong (>10 m/sec) wind events.

function of frequency. When plotted the spectrum gives a concise picture of the frequency distribution of the kinetic energy (variance). Of course, the characteristics that showed clearly on other plots should also be evident in the spectral plots.

Calculating the spectrum for one series (autospectrum) can be useful, but this can also be done for two records (cross spectrum). Normalizing such a spectrum by the variances produces a "coherence" as a function of frequency. The coherence is the frequency-dependent counterpart of the correlation function between two series as a function of time lag; instead of showing the time lags at which records are correlated, it shows the frequencies at which records are phase locked (the calculation also yields the corresponding phase spectrum, a frequency-dependent time difference). We plot the square of coherence because, like the squared correlation coefficient, the squared coherence corresponds to the percent of the variance at the frequency that is "explained" by a linear relationship. Coherence is always positive, but phase information (not shown) conveys sign. For instance, two sine waves of identical frequency but opposite sign have a coherence of 1.0 and a phase of 180°.

We illustrate with examples that summarize the frequency distribution of kinetic energy over the shelf. Autospectra for BC-15C, 20 m and 34 m depth, from summer 1977 are plotted in Fig. 5-5. The vertical axis is kinetic energy *density*, i.e., per unit frequency, $(cm/sec)^2$ /CPD (CPD is cycles per day). In this presentation the vector series have been decomposed into clockwise (anticyclonic) and counterclockwise (cyclonic) rotating components, instead of into north-south and east-west components. When there is no strong local orientation (e.g., a shoreline or strong bathymetric gradient), the clockwise/counterclockwise decomposition is more useful than the east/north decomposition. The most striking feature of both records is the high diurnal (1 CPD) and semidiurnal (2 CPD) peaks, with the semidiurnal higher. This conforms to our knowledge that motion over the shelf is tidally dominated (cf. Figs. 5-2 and 5-3). For the shallow record 89 percent of the energy was tidal (70 percent semidiurnal) and for the deeper record 94 percent was tidal (67 percent semidiurnal). At low frequencies there were small irregular peaks. This also corresponds to expectation, as the low-frequency filtered records did not reveal any dominant frequencies (cf. Fig. 5-4). Near the inertial frequency (1.7 CPD), in the clockwise components only, there is a small, statistically insignificant peak. One characteristic of inertial

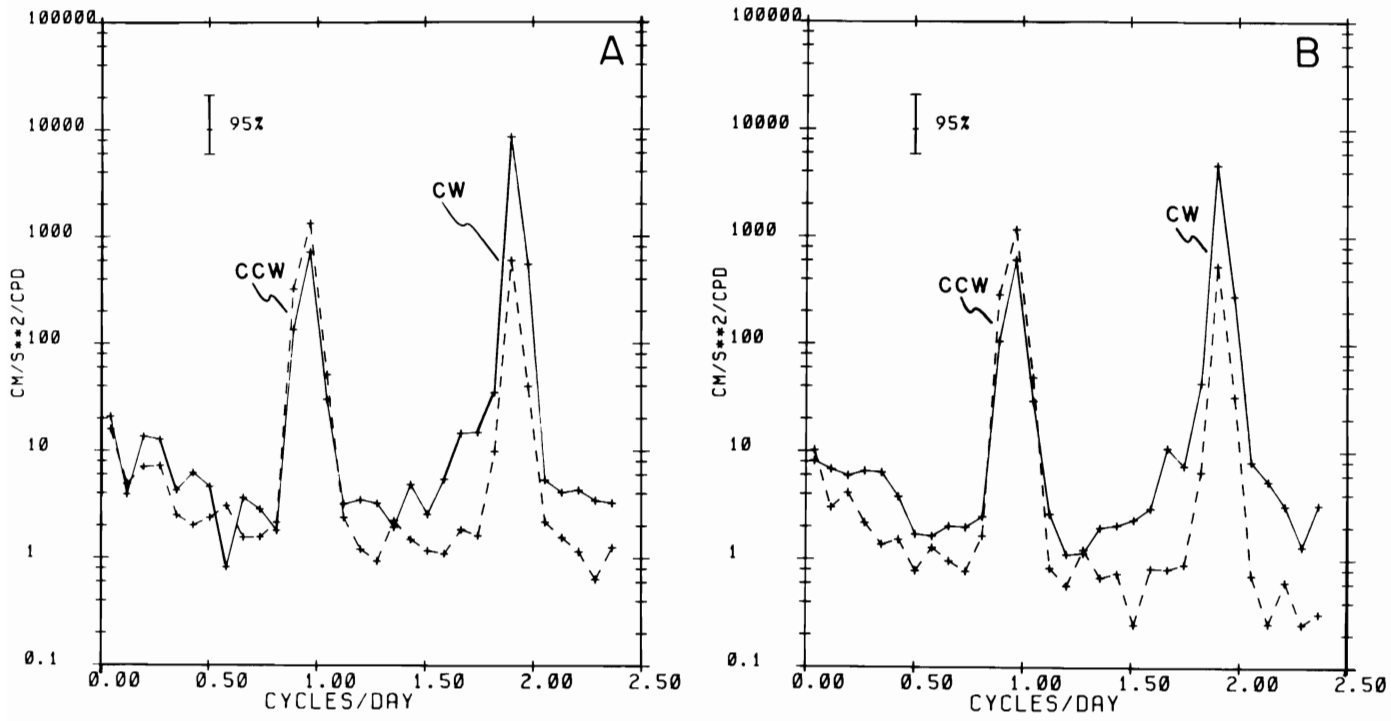

Figure 5-5. Autospectra, BC-15C 20 m and 34 m. The energy density (cm^2 sec^{-2} CPD^{-1}) versus cycles per day shows strong diurnal and semidiurnal tidal peaks, and irregular low-frequency peaks. Clockwise (solid) and counterclockwise (dashed) current components are plotted.

oscillations (in the Northern Hemisphere) is clockwise rotation, and the presence of similar peaks near the inertial frequency in most records has led us to label these peaks inertial. An example of vertical coherence from mooring 5A at 20 m and 50 m depth during summer 1976 is shown in Fig. 5-6. Again, we used clockwise and counterclockwise components. Not surprisingly, the tidal peaks show clearly. Tidal motion at 20 m depth was coherent with motion at 50 m depth. In our records vertical coherence >0.9 at tidal frequencies was common, and since most of the energy was at tidal frequencies, this implies that shallow and deep motions were generally coherent. As with most of the records there are also some low-frequency peaks above the 95 percent confidence limit (~ 0.26). Examining individual records (plotted versus time), we often found that shallow and deep records were highly correlated during strong winds, but over the entire record low-frequency flow was often weak and uncorrelated. This is consistent with coherence estimates like that in Fig. 5-6.

In general then, we find that motion throughout the sampled water column was highly coherent at tidal frequencies, and either weakly coherent or not coherent at other frequencies. When the coherence was high, the phase differences were usually small, so that the flow at these frequencies was in the same direction at both depths. During strong winds, the low-frequency flow was vertically correlated (see below, Seasonal Variations and Meteorological Forcing) and this probably caused the occasional peaks in coherence at low frequencies. Coherence calculations do not reveal relative speeds, but an examination of Table 5-1 shows that shallow instruments usually recorded faster speeds than deeper ones. This may be instrumental (see Introduction) or it may reflect an actual decrease with depth.

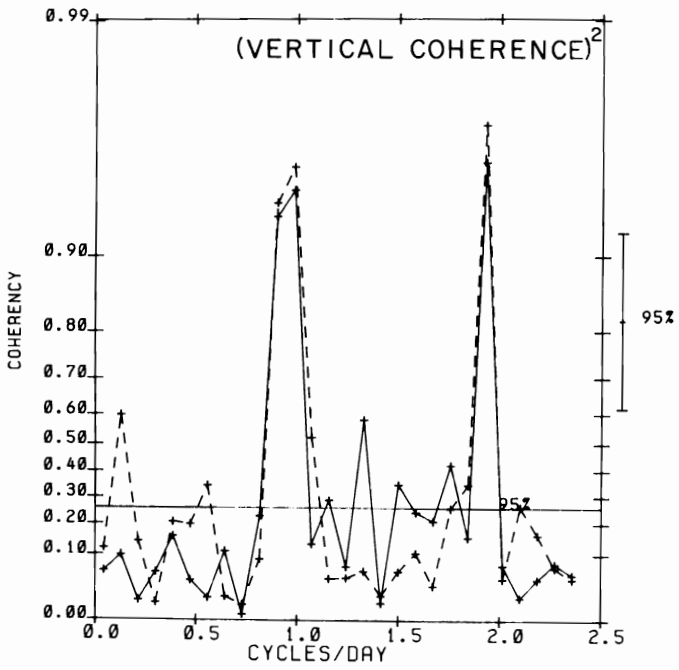

Figure 5-6. Vertical coherence squared. The squared coherence of BC-5A 20 m with BC-5A 50 m is shown, in clockwise (solid) and counterclockwise (dashed) components. Highly significant coherences in tidal bands are common to all records. Some also show strong low-frequency coherence and inertial (1.7 CPD, clockwise) coherence.

Just as it is possible to calculate the vertical coherence to help determine whether motions are similar throughout the water column, horizontal coherences calculated between records from different moorings help determine if motions are similar over broad areas. The low-frequency sticks in data from July 1976 suggested to us that the water motion at low frequencies might be coherent over part of the shelf (see Fig. 5-10); we calculated coherence between BC-5A (50 m), BC-2C (20 m), and BC-6A (50 m). The deep instrument on mooring BC-2C failed, but the current meter at a nominal depth of 20 m was below the pycnocline. Calculations between these instruments showed coherence at separations of 30, 42, and 72 km. Again, the calculated tidal coherences squared exceeded 0.9 (Fig. 5-7). At low frequencies there was also high coherence squared in a broad peak which decreased with separation: at 30 km it was ~ 0.7, and at 72 km it was ~ 0.55. These peaks suggested that the middle shelf was similarly affected by low-frequency motions, and probably most of these motions were generated by wind events similar to those discussed under Seasonal Variations and Meteorological Forcing. Values of coherence squared between the middle shelf and coastal records at comparable distances (~ 60 km) were lower (~ 0.4), but still significant.

MEAN CIRCULATION

Although the kinetic energy distributions were dominated by tidal currents, many of the records had significant means (e.g., Fig. 5-3A). We examine the statistical significance of the record means, and construct a circulation scheme using them. The mean flow is energetically two orders of magnitude smaller than the tidal flow over much of the shelf, however, and the mean circulation may not be the most important flow component in many situations.

A vivid example is the flow through the Aleutian

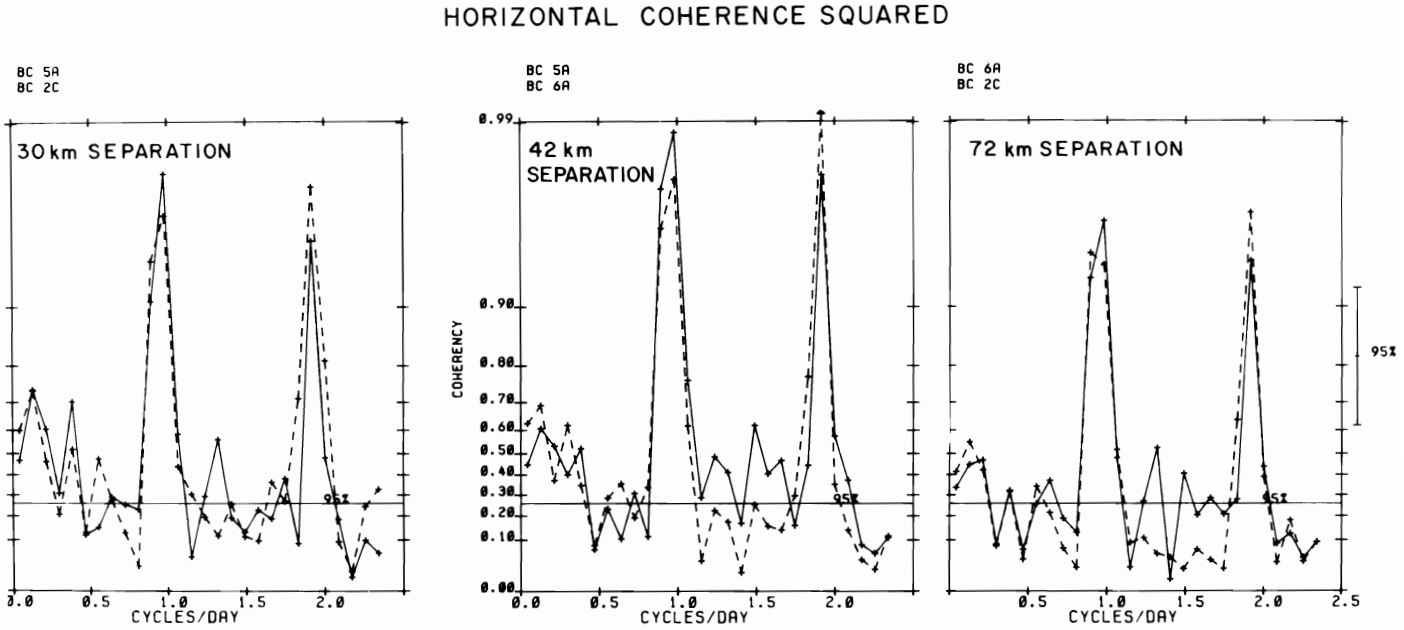

Figure 5-7. Horizontal coherence squared. Even at a separation of 72 km, low-frequency (~0.3 CPD) coherence squared is nearly 0.6, and at 30 km it exceeds 0.7. The horizontal coherence was higher over the middle shelf (shown here) than in the coastal or outer regimes. Clockwise components have solid lines.

Passes (such as Unimak Pass). Flows in many of these passes have high mean scalar speeds, exceeding 100 cm/sec (see U.S.D.C. 1964), but these are mostly caused by tidal currents and may average to a vector mean of zero. Properties (e.g., salt and drift cards) can be exchanged between the North Pacific and Bering Sea through such a pass; it is unlikely that the same volume of water flows back and forth on ebb and flood, and the vigorous stirring near coast and bottom prevents such a volume of water from remaining intact. Practically, it is difficult to measure the mean flow in such passes with present techniques. For many oceanographic questions, the mean flow is not as important as the exchange of properties between two oceanic regimes and the mixing by vigorous tidal stirring.[4]

Just as obviously, the mean circulation over the Bering Sea shelf, even if much smaller than the tidal currents, can importantly influence many processes. For instance, plankton advected by a 2 cm/sec vector mean flow would travel about 150 km over the summer. Such a small mean flow is difficult to measure in a highly variable and active (noisy) background. The 2 cm/sec mean flow may be important, but separating it from the tidal and other variable currents with statistical significance requires measurements of long duration. For example, we had six different moorings at location BC-4 (Fig. 5-1), and for each mooring we computed a mean (Table 5-1) from records 45-209 days long, and instruments 18-52 m deep. These means accounted for less than 1 percent of the horizontal kinetic energy in this tidally dominated flow. All means fell in the northwestern quadrant, varying from 274 to 311°T with speeds from 0.4 to 3.6 cm/sec. The unweighted means for these records (± one standard deviation) were: 2.1 ± 1.2 cm/sec and 301 ± 11°T. Although we cannot compare this to the actual mean, the repeatability gives us confidence in our data. Some of the variability was not due to measurement error: seasonal differences (wind stress, ice cover, and stratification), vertical velocity shear (the means of shallow records averaged 1.2 cm/sec faster than the deeper ones), and interannual changes accounted for some variation.

A reasonable qualitative estimate of the significance of the mean flow can be inferred from progressive vector diagrams (Fig. 5-3). To quantitatively estimate the statistical significance of the means, we used low-pass (35-hour) filtered records. We define a time scale[5] (Υ) of the low-frequency flow and then estimate the number of independent samples of the mean by dividing into total record length (T). Thus an estimate of the error (at 67 percent confidence) is:

[4] Mean flow is often assumed through Unimak Pass into the Bering Sea; we know no evidence for this, only for an exchange between the Bering and the North Pacific.

[5] The time scale is estimated by computing the area under the autocorrelation function; it is thus twice the "integral time scale" (Kundu and Allen 1976).

$$E = \frac{\sigma}{(T/\Upsilon)^{1/2}}$$

E: root mean square error estimate (cm/sec)

σ: standard deviation of record (after low-pass filtering; cm/sec)

T: record length (sec)

Υ: time scale (sec), the length of an independent sample.

An example of these calculations is given in Table 5-4, illustrating the significance of means for summer 1976. For these records, the mean was usually significant in the coastal regime, where it was about three times the estimated error. Over the middle shelf, however, the mean was generally equal to or less than the standard error. In the outer regime, the mean was much greater than the error. These examples conform to a general pattern: in the outer regime, means were greater than errors, in the coastal regime means were somewhat greater than errors, and in the middle regime means were insignificant. This generalization must be modified for measurements taken just seaward of the inner front separating the coastal and middle hydrographic domains (e.g., BC-4, Fig. 5-1). Such measurements show significant means because of their proximity to the front. These measurements also illustrate that the boundaries of the flow regimes nearly coincide with those of the hydrographic domains, but not exactly.

TABLE 5-4

Means and standard errors

Record	U± Eu (cm/sec)	V± Ev (cm/sec)	S, E[1]
Coastal			
BC-15A (20 m)	−2.3 ± 0.3	0.1 ± 0.5	2.3, 0.6
BC-14A (20 m)	3.3 ± 0.4	1.2 ± 1.0	3.5, 1.1
(40 m)	−0.4 ± 0.4	−0.6 ± 0.4	0.7, 0.6
Middle			
BC-2C (20 m)	0.4 ± 0.4	0.6 ± 0.3	0.7, 0.5
BC-5A (20 m)	−0.1 ± 0.5	−0.5 ± 0.4	0.5, 0.7
(50 m)	−0.1 ± 0.3	0.1 ± 0.7	0.1, 0.8
BC-6A (20 m)	0.6 ± 0.6	0.2 ± 0.4	0.6, 0.7
(50 m)	0.6 ± 0.4	0.8 ± 0.4	1.0, 0.6
Outer			
BC-17A (96 m)	−2.9 ± 0.1	1.4 ± 0.4	3.2, 0.4
BC-13C (22 m)	−2.4 ± 1.9	4.7 ± 1.5	5.3, 2.4

U and V are the record means, and Eu and Ev are the estimated standard errors (see text). S and E are the vector mean speed and the vector sum of the errors.

[1] $S = (\bar{U}^2 + \bar{V}^2)^{1/2}$ $E = (Eu^2 + Ev^2)^{1/2}$

Computed means for each mooring location (Fig. 5-8) show the general circulation pattern. Over the entire shelf, significant mean flow usually paralleled local isobaths. In the outer regime mean flow was parallel to the shelf break, flowing northwestward at 1-5 cm/sec. In the middle regime mean flow was insignificant, usually <1 cm/sec. In the coastal regime between Cape Newenham and Nunivak Island flow was westward at 1-3 cm/sec, while along the Alaska Peninsula flow paralleled the nearby shoreline at 2-5 cm/sec.

Drifters, tracked by satellite, provided confirmation of flow character in the outer and middle regimes. Three drifters launched in June 1976 (near BC-2, -5, and -6) confirmed low vector mean speeds there, <1 cm/sec in the absence of strong winds. In 1977, six drifters released over the continental slope in the outer and oceanic regimes all drifted northwestward with vector mean speeds ~5 cm/sec (Coachman and Charnell 1979, Kinder et al. 1980). Two of these drifters wandered into the middle regime near the Pribilofs, where their vector mean speed was ~1 cm/sec. These drifters gave no evidence of exchange across the shelf break (i.e., crossing the front overlying the continental slope, Kinder and Coachman 1978), except in the area just north of the Alaska Peninsula.

Kinder et al. (1978) found water lying along the Alaska Peninsula below 20 m that was both warmer and more saline than surrounding waters. Muench and Ahlnäs (1976) noted that the region just north of the Alaska Peninsula was often free of ice when nearby water was ice-covered. These distributions could result from the advection of warmer oceanic water onto the shelf north of the peninsula. Moreover, one of the drifters deployed over the slope in 1977 crossed the shelf break north of the Unimak Pass, and traveled about 80 km eastward before grounding on the peninsula (Kinder et al. 1980).

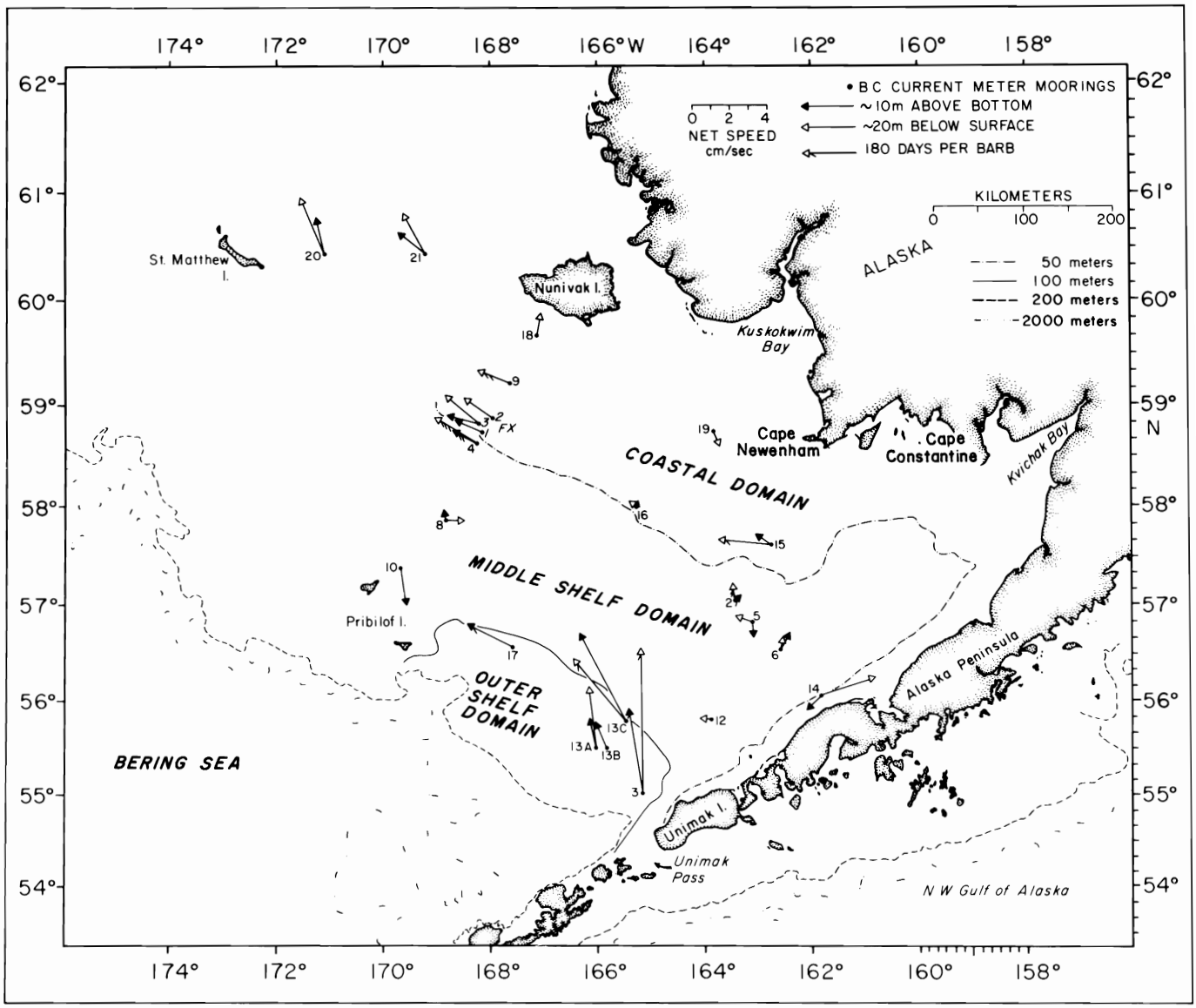

Figure 5-8. Mean flow. The mean for all records at each mooring site is shown. Coastal and outer regime moorings generally had statistically significant means, while middle shelf sites did not. The domains refer to hydrographic structure (preceding chapter), but the domains and flow regimes are nearly coincident.

These measurements are strong evidence for flow across the shelf break near the Alaska Peninsula (note BC-14, Fig. 5-8), but hydrographic and current measurements also demonstrated that this flow is probably intermittent.

Mean flow over both the outer and coastal regimes appeared to be driven by pressure gradients caused by density differences. The method of inferring flow from dynamic calculations, referred to the deepest common depth of nearby hydrographic stations, gave approximate agreement with direct measurements (Coachman and Charnell 1979, Schumacher et al. 1979). Dynamic topographies in the outer regime (Kinder 1977, Coachman and Charnell 1979, Kinder et al. 1978) indicated westward flow of ~5 cm/sec. Calculations across the inner front (near the 50 m isobath) yielded 1-2 cm/sec flow counterclockwise along the front and westward between Cape Newenham and Nunivak Island (Schumacher et al. 1979). Thus mean flow in both the outer and coastal regimes can be inferred from the density field, but this is not true of the middle shelf, where the mean is nearly zero. Dynamic topographies do suggest a very weak southeastward flow across the middle regime (e.g., Kinder 1977, Reed 1978, and Kinder et al. 1978), but the current records (Fig. 5-8) did not confirm this flow.

Synthesizing our knowledge of the shelf circu-

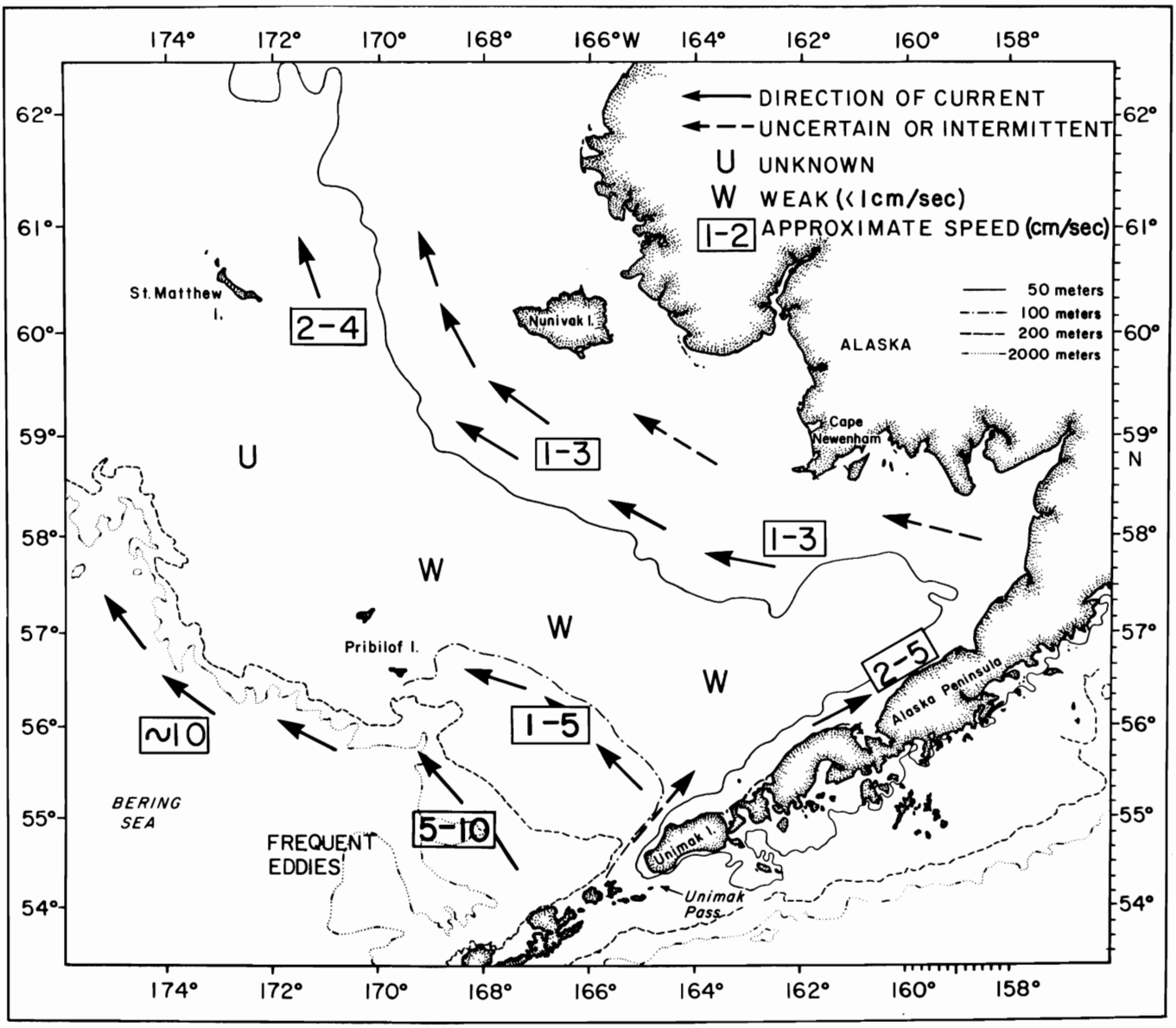

Figure 5-9. Estimated mean circulation. No strong distinction is made as to season or depth, although it is biased toward summer and the surface. The dashed arrows in the northern coastal regime express uncertainty, while the arrow along the Alaska Peninsula expresses intermittency. Flow over the shelf is mostly tidal, so that the instantaneous flow is quite different from this depiction. For instance, over the middle shelf we expect the speed at any time to exceed 20 cm/sec even though the long-term vector mean is less than 1 cm/sec, and instantaneous directions seldom agree with the arrows at any location. The scheme is also incomplete: the source of water for the westward transport in the coastal regime is not shown. We speculate about this source in the text.

lation, we have constructed a circulation scheme (Fig. 5-9). We emphasize again that the mean circulation is only a few percent of the total kinetic energy, and that even our large data sets do not define the mean flow adequately at some locations. That is, the arrows in Fig. 5-9 will often be incorrect instantaneously and scalar speeds will be much higher than the long-term vector means. Directions apply throughout the water column and speeds at the surface; speeds decrease significantly with depth seaward of the 100 m isobath. Our data are most extensive in summer (Table 5-1), but most data from other seasons agreed with this depiction.

In the coastal regime we show counterclockwise flow extending northward to St. Matthew Island with speeds of a few cm/sec. Within Kvichak and Bristol bays, measurements show that the counterclockwise flow extends to the coast (Straty 1977). The dashed arrow paralleling the Alaska Peninsula signifies intermittent flow. In the middle regime we show

weak mean flow (<1 cm/sec), direction indeterminate. In the outer regime and over the slope we show strong (1-10 cm/sec) flow paralleling the shelf break and flowing westward. Wherever the flow was well defined, the entire water column moved in the same direction, but speed decreased significantly with depth in the deeper water seaward of the shelf break. This flow is a continuation of eastward flow north of the Aleutian Islands which then curves cyclonically toward the west in the southeastern corner of the deep Bering Sea (Kinder et al. 1980). We also note that eddies seem to be common over the deeper water, so that "mean" currents there may radically change direction for weeks or months (Kinder and Coachman 1977, Kinder et al. 1980). We have not observed comparable eddies in the shelf waters.

We found no evidence of large flow onto the shelf; the flow leaving the shelf to the west in the coastal regime should also have small volumetric transport. We can estimate this outflow by assuming a 2 cm/sec flow over an average depth of 25 m along a section 150 km long, approximating conditions southwest of Nunivak Island to the inner front (i.e., spanning the coastal regime). This transport is 2 cm/sec $\times$ 25 m $\times$ 150 km = 0.08×10^6 m^3/sec, or less than 10 percent of the Bering Strait outflow ($\sim 1 \times 10^6$ m^3/sec), but still larger than the river runoff (0.0015×10^6 m^3/sec: Roden 1967). Water to supply this westward flow may come from the middle shelf; across the middle regime, between the front and the Pribilofs, a southeastward transport of 0.08×10^6 m^3/sec across 200 km averaging 70 m deep would be only 0.5 cm/sec, detectable in neither our current nor our hydrographic data. Inflow along the coastal regime north of the Alaska Peninsula (30 km wide by 25 m deep) would need to be a steady 10 cm/sec, which is not supported by data, although some lesser inflow does occur there.

Thus the circulation scheme shown in Fig. 5-9 is incomplete because the source of water necessary to supply the westward transport in the coastal regime is not shown. We conjecture that this supply is mostly from the shelf northwest of our study region and that it flows southeastward into the middle regime. It may then enter the coastal regime in Bristol Bay, where the inner front appears weakest (see Chapter 4). Since the evidence for this circulation is weak, we exclude it from Fig. 5-9.

SEASONAL VARIATIONS AND METEOROLOGICAL FORCING

Some characteristics of the shelf environment change annually: insolation, river runoff, ice cover, wind stress, and atmospheric pressure. Even though the tides, which have little seasonal variation (Pearson et al., Chapter 8, this volume), force most of the current, seasonal variation occurs in the non-tidal currents. These seasonal changes are small but still significant.

We showed some of the hydrographic changes in the preceding chapter. An example of changes in atmospheric forcing is shown in Table 5-5 (see also Overland and Niebauer, Chapters 2 and 3, this volume). During the winter, mean wind speeds are higher and storms are more frequent. Stratification is much weaker over most of the shelf, and we might thus expect more direct response to the wind in the absence of ice cover, which may alter the effect of the wind stress. Records from BC-2 and BC-9 indicate some seasonal changes, even when allowance is made for instrumental problems from more energetic surface waves (Table 5-6). Seasonal changes that we describe exceed the 25-30 percent error estimates (see Introduction).[6]

At BC-9 the shallow summer mean was 1.0 cm/sec toward 316°T. Decreasing the winter mean by one-third (a high estimate of the false inflation of speed by surface waves), the mean was 3.2 cm/sec toward 315°T. Likewise, BC-4 had higher vector mean speeds during winter, with the same direction as in summer. Another site with sufficient data to suggest

TABLE 5-5

St. Paul weather 1975-76

	Mean pressure (mbar)	Mean speed (m/sec)	Variance (m^2/sec^2)	Vector mean (m/sec, °)
Summer 1976	1011	6.2	43	1.3 at 004
Winter 1975-76	1006	8.5	85	2.4 at 202

The weather station on St. Paul Island (northernmost of the Pribilofs) probably represents weather over the southeastern shelf better than the other stations, which are strongly influenced by topography.

[6] The seasonal differences are slightly different from what might be inferred from Tables 5-1 and 5-3 because: Tables 5-1 and 5-3 use entire record lengths instead of smaller seasonal segments and we examine the meteorological frequency band (1.5-10 day) for seasonal effects, a subset of the low-frequency category in Table 5-3. A sequential 29-day tidal harmonic analysis was used to estimate errors in the Introduction, whereas Table 5-6 lists wide-band tidal estimates (identical with Table 5-3).

TABLE 5-6

Seasonal kinetic energy (cm^2/sec^2)

Record	Season	Fluctuating	Low[1]	Semidiurnal	Meteorological[1]
Coastal					
BC-9C 23 m	Summer 5/12-9/10/77	340	6	256	4
BC-9B 23 m	Winter 9/24/76-5/12/77	434	59	271	47
Middle					
BC-2C 20 m	Summer 5/31-9/26/76	175	3	110	2
BC-2B 50 m	Winter 11/5/75-5/14/76	203	11	120	7
Outer					
BC-3C 20 m	Summer 5/29-9/28/76	510	149	251	74
BC-3C 100 m	Summer 5/29-9/28/76	266	30	165	21
BC-3A 20 m	Winter 11/7/75-3/16/76	511	112	285	69

[1] Low-frequency energy includes all subtidal (less than diurnal frequency) energy in the record. Meteorological frequency energy is only that within the 1.5-10 day (0.67-0.10 CPD) band.

Note the relative constancy of the semidiurnal tidal energy at each mooring site.

seasonal changes is BC-2. Like BC-9 and BC-4, currents at BC-2 were faster in winter, with a vector mean speed (~1.5 cm/sec) about double the summer value. Unlike the other two sites, however, at BC-2 the direction reversed from westward (~300°T) in summer to eastward in winter.

The kinetic energy spectra showed that the greatest relative change occurred in the meteorological band, between 1.5 and 10 days (Table 5-6). This band corresponds to the increased variance seen in St. Paul wind data (Table 5-5). In the middle regime a record for 20 m in the summer of 1976 (BC-2) had meteorological kinetic energy of 2 cm^2/sec^2, while the deep 50 m record was threefold greater in the winter of 1976-77—7 cm^2/sec^2. In the coastal regime 23 m records (BC-9) showed greater differences between seasons. In summer 1977 meteorological band variance was 4 cm^2/sec^2, but during the winter of 1976-77 it was 47 cm^2/sec^2. These changes for the middle and coastal regimes exceeded our error estimates, but changes in the outer regime (BC-3) did not. This reinforces the idea that subtidal energy in the middle and coastal regimes is mostly meteorologically forced, while low-frequency energy in the outer domain is not forced by local weather. In the outer regime, the low-frequency energy is probably associated with variations in the Bering Slope Current.

Two different meteorological conditions can force low-frequency current pulses. One dominates the summer pulses and the second occurs only in winter. The summer condition is an eastward-moving low atmospheric pressure center, and the winter condition

is a southward outbreak of cold continental air. Strong storms associated with atmospheric low-pressure cells also occur in other seasons, but the continental air outbreak is exclusively a wintertime phenomenon.

Such a summer event occurred in late July 1976 when several current-meter moorings and drifters were placed in a line running northwest from the Alaska Peninsula (Fig. 5-10). (We suspect biological fouling of the upper instruments, especially BC-5 (20 m) and BC-6 (20 m), so that speeds in some records are too low.[7]) As the wind increased to 10 m/sec and rotated towards the east, currents at moorings 5, 6, and 2 responded similarly, with about a one-day lag. That is, speeds increased, and direction rotated slightly clockwise toward the east after peak speeds were reached. The shallow current meter at mooring 14 showed a similar speed increase, but direction remained essentially parallel to the local bathymetric contours (Figs. 5-1 and 5-8). The two drifters still operating at that time had shown aimless wandering at mean speeds <1 cm/sec before the strong winds began. They were still near the moored instruments in late July (they were launched in early June), and responded strongly during this event. Both drifters accelerated to speeds near 20 cm/sec, and changed directions clockwise toward the east.

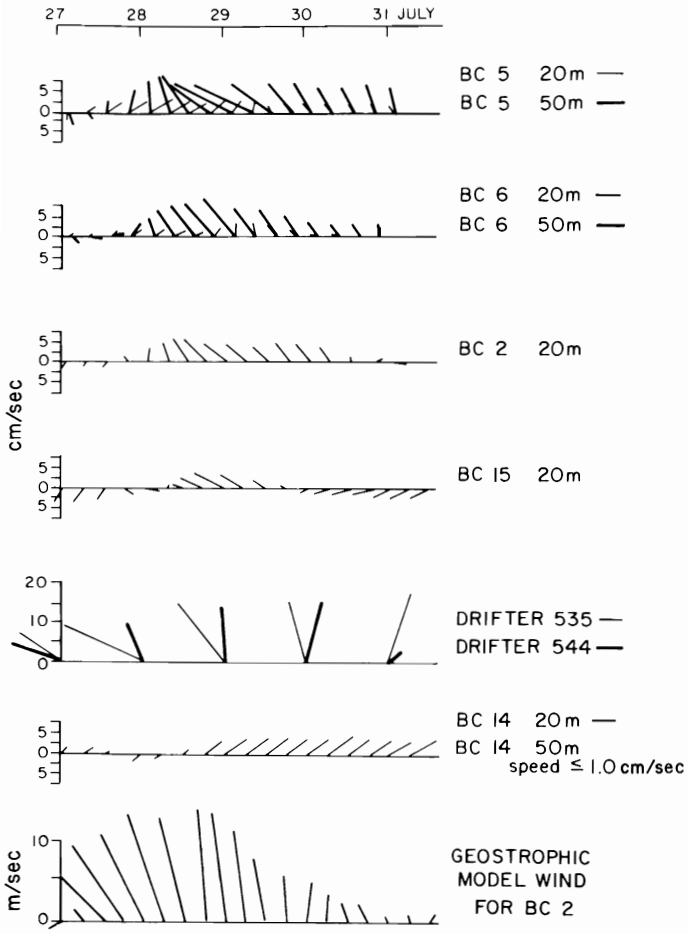

Figure 5-10. Current response to a summer wind event, middle and coastal regimes. Stick diagrams for current meters, drogued drifters tracked by satellite, and estimated wind. As the wind increased beginning on 27 July 1976, currents also increased and followed the wind in a clockwise rotation. Biological fouling probably decreased speeds at BC-5 20 m and BC-6 20 m.

[7] In Chapter 28, F. Favorite cites an 1894 report of jellyfish fouling fishing gear near the Alaska Peninsula. Our fouling problem in the same area was also caused by jellyfish.

The current pulse illustrated by Fig. 5-10 was typical of many similar pulses in the current records, and is the best documented such event. These pulses also seem characteristic of the low-frequency currents in the two nearshore regimes. In our records, 50 percent of the low-frequency (subtidal) variance lies in the band 0.7-0.1 cycles per day (1.5-10-day period), which includes the repetition rate for storms.

The continental air outbreak, which occurs frequently in winter, apparently affects both the currents and ice distribution (see preceding chapter). High pressure over the Alaska mainland results in an offshore wind of cold, dry air blowing southward off the ice. This type of weather permits excellent satellite imagery (Fig. 5-11; see also Muench and Charnell 1977). Crossing the southern ice boundary, the cold, dry air receives heat and moisture from the underlying water. Clouds form downstream from the ice edge as long (hundreds of km) streamers paralleling the wind.

A record from BC-2B (Fig. 5-12) concurrent with a southward outbreak of cold continental air showed a strong (20 cm/sec) current pulse to the south during the period 19-22 January 1976. As the satellite image shows, winds were blowing SSE near BC-2 by 20 January in excess of 20 m/sec, and rotated slightly from south to south-southeast (cf. Fig. 5-10). Similar pulses were observed during winter 1977 at BC-2. In January, a five-day pulse averaged 15 cm/sec to the southeast and in February flow exceeded 30 cm/sec to the northeast for 30 hours.

Within the two inner regimes, winter brought energetic response to meteorological forcing (Table 5-6). Mean winds were stronger then (in the absence of storms), and strong winds occurred more frequently. Although the tides still dominated energy spectra, energy at meteorological frequencies played an increasing role, leading to the reversal of mean flow at BC-2. Ice cover probably modifies this forcing, but even under the ice (BC-9) wintertime winds cause current responses.

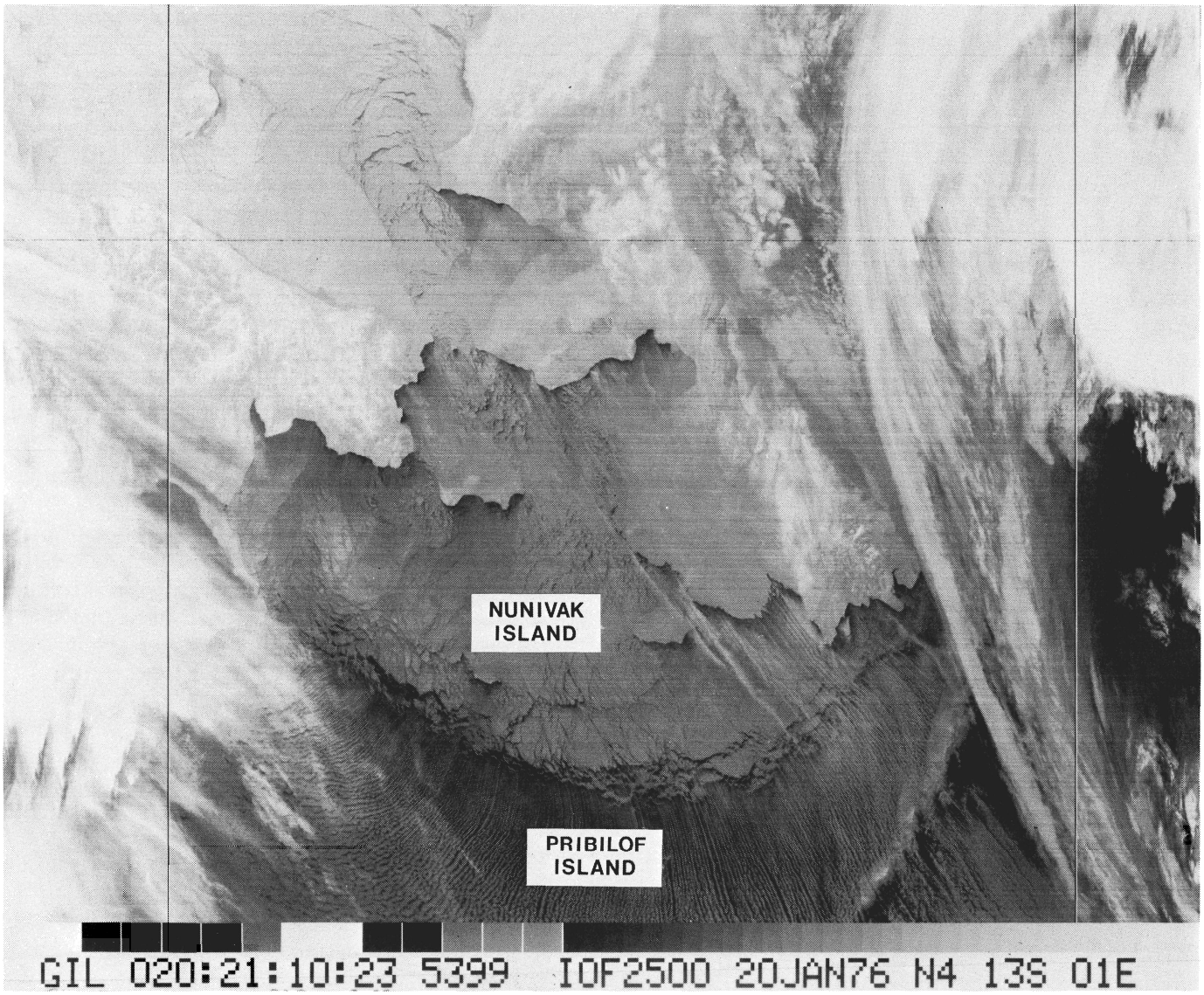

Figure 5-11. An infrared satellite image of the Bering Sea on 20 January 1976. The Alaska Peninsula, Pribilof Islands, Nunivak Island, and other land features show clearly. The ice pack extended south of Nunivak Island, with some typical lineations, mostly tending east-west and parallel to the ice front, near the edge of the ice. Thin streamer clouds, normal to the ice front and parallel to the wind, extended southward. Fig. 5-12 shows measured currents and estimated winds.

FLOW REGIMES AND HYDROGRAPHIC DOMAINS

We have used flow regimes as a framework for discussion in the preceding sections, and now we summarize their characteristics (Table 5-7). As with the nearly coincident hydrographic domains (preceding chapter), our description is biased toward summer. The discussion of seasonal variation showed, however, that many of the differences between regimes persist throughout the year.

Energy of the fluctuating flow was 90 percent tidal over the middle shelf, about 80 percent in the coastal regime, but only 60-70 percent in the outer regime, where up to 30 percent of the energy was at periods greater than two days (Table 5-3). Inertial energy was about 1 percent of the energy in the outer regime, but barely detectable in the two shoreward regimes. The increase in tidal energy per unit mass in these two regimes is a consequence of shoaling. Larger fluctuating kinetic energy values at low frequencies in the outer regime probably reflect variability of the persistent westward-flowing current there. Oceanic currents usually have unsteady components with periods of a few days or longer.

Spatial differences also appeared in coherence

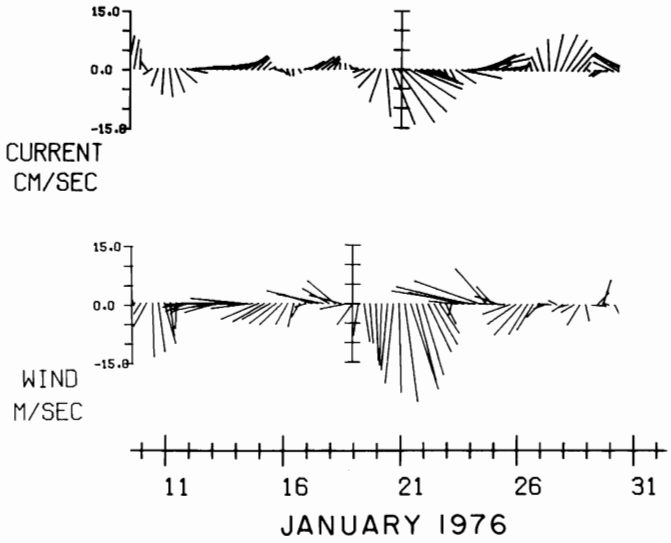

Figure 5-12. Low-pass (35-hour) filtered current (upper, cm/sec) and wind (lower, m/sec), from BC-2B 50 m. The wind data are from Fleet Numerical Weather Central estimates. Note the strong wind-driven pulse to the south during 19-23 January. Fig. 5-11 shows concurrent wind and ice conditions.

calculations. Vertical coherence was significant at tidal frequencies everywhere, but at low frequencies only in the coastal regime, perhaps because the water column there is homogeneous, unlike the other two regimes, which have strong stratification (during summer). This stratification may confine responses (e.g., to wind events) to only part of the water column. Horizontally, tidal coherences were large everywhere. Significant low-frequency squared coherences (~0.6 at 70 km separation) existed over the middle shelf during the summer of 1976, but were lower (~0.4) at similar distances between the middle and coastal regimes (i.e., across the inner front). Coherence squared was low in the outer regime and in the coastal regime, except at tidal frequencies (the number of records and their separations make this a tentative conclusion). The high coherence in the middle regime may be caused by the low background —the amount of low-frequency energy was small, and was mostly forced by wind events which have large spatial scales. Other processes may cause low-frequency motions in the outer and coastal regimes, and these competing processes can lower coherences calculated over long records.

At low frequencies the clear meteorologically driven pulses, as illustrated in Figs. 5-10 and 5-12, were observed only over the middle shelf. Some vestige of these was seen in coastal records, but not in the outer regime. It may be that the response to these wind events is so weak that it is swamped in the regimes with more low-frequency energy (coastal and outer, see Table 5-3), but not in the middle regime.

These spatial changes in flow thus occur at many frequencies: tidal, subtidal, and mean (see preceding section). They are nearly congruent with hydrographic domains, so that the fronts delimiting these domains also bound flow regimes. Some of the relationship between the hydrographic domains and the flow regimes is clear. In the outer regime the mean flow agrees with the dynamic topography, as is true in the coastal regime and near the inner front. Variations in response to wind forcing are less clear, but are probably related to the changes in stratification and water depth.

SUMMARY

With a preliminary analysis, we have characterized the flow over the southeastern Bering Sea shelf. The spatial and temporal coverage of the measurements were perhaps two orders of magnitude better than previously available. We have calculated the frequency distribution of the flow, defined the separation of the shelf into three regimes, suggested annual variations, and identified meteorological forcing.

Flow above this shelf was mostly tidal: the scalar mean tidal speeds were about 20-25 cm/sec, increasing shoreward. About 80 percent of the tidal energy was semidiurnal (see Chapter 8, this volume). For individual records, up to 95 percent of the fluctuating energy was tidal, but both subtidal fluctuations and (record) means were significant. Differences in these low-frequency and mean flows defined distinct flow regimes nearly coincident with previously defined hydrographic domains (see preceding chapter).

In the outer regime, between the shelf break and the 100 m isobath, mean flow was westward at 1-5 cm/sec, agreeing with the dynamic topography. Energy at subtidal frequencies appeared unrelated to local meteorology, and may have resulted from oscillations of the Bering Slope Current and the associated front overlying the continental slope. Farther inshore, between the 100 m and 50 m isobaths, the middle regime had insignificant mean flow (although vigorous tidal currents exceeded 20 cm/sec). Near the inner front mean flows existed, however, at speeds of 1-5 cm/sec parallel to the 50 m isobath in a counterclockwise sense similar to calculations of geostrophic flow across the inner front. North of the Alaska Peninsula there appeared to be a net eastward flow during summer, but it seemed to be intermittent.

Ice cover and winds vary annually, and changes in flow were discernible over the seasons. In summer,

TABLE 5-7

Flow regimes

	Outer	Middle	Coastal
Fluctuating horizontal kinetic energy	60-70% tidal 1% inertial	90% tidal inertial (?)	80% tidal inertial (?)
Vertical coherence[1]	only tidal	only tidal	tidal and low frequency
Horizontal coherence[1]	only tidal	tidal and low frequency (C^2 ~0.7 @60 km)	only tidal
Wind events	obscure	clearly present	present
Mean[3]	1-5 cm/sec westward geostrophic balance	0.5 cm/sec random Note[2]	1-5 cm/sec counter-clockwise geostrophic balance

[1] The characteristics of coherence are particularly tentative. Missing records, improperly positioned instruments (e.g., both current meters on the same mooring in lower layer), and poor spatial coverage prevent strong conclusions. (C^2 is coherence squared.)

[2] In the vicinity of the inner front (near the 50 m isobath) speeds are 2-5 cm/sec and parallel the isobath (along-frontal) in a counterclockwise sense.

[3] Also see Figs. 5-9 and 5-10.

storms are less frequent and winds (in the absence of storms) are generally weaker (Chapter 3, this volume) than in winter. Currents directly driven by the wind were stronger and more common in winter than in summer within the coastal and middle regimes, but were not detectable in the outer regime in either season.

Further analysis of data already collected will make the description of shelf circulation more complete. Moreover, progress will be made in understanding the dynamics of the shelf circulation and its interactions with the variations in hydrographic structure across the shelf with the help of clues from more detailed examination of annual changes. Annually the mean wind stress, the wind stress variance, the stratification and its horizontal variation, the horizontal density (salinity) gradient, the freshwater discharge from rivers, and the extent of ice cover all undergo great changes. Understanding the effects of these on the circulation of this shelf will increase our understanding of shelf dynamics in general, and help us to understand the ecosystem of the Bering shelf.

ACKNOWLEDGMENTS

Many people contributed to the work reported here, and we list only those who directly helped us prepare reports or manuscripts: L. K. Coachman, D. V. Hansen, R. L. Charnell, R. B. Tripp, D. J. Pashinski, J. C. Haslett, N. P. Laird, R. L. Sillcox, and K. Ahlnäs. L. K. Coachman was principal investigator with us during this project. There was also a small army of engineers, technicians, computer specialists, and secretaries at the University of Washington, Pacific Marine Environmental Laboratory, and Naval Ocean Research and Development Activity whose efforts made this report possible. The officers and crews of *Acona*, *Moana Wave*, *Discoverer*, *Surveyor*, and *Miller Freeman* spent many uncomfortable hours at sea supporting the field program. L.K. Coachman,

J.R. Holbrook, and three reviewers made many helpful criticisms of this chapter.

Funding came from the Outer Continental Shelf Environmental Assessment Program, which is administered by the National Oceanic and Atmospheric Administration for the Bureau of Land Management. This is PMEL contribution number 426. While writing this paper, T. H. Kinder was supported by the Naval Ocean Research and Development Activity.

Bob Charnell was a co-principal investigator on this project, and Pat Laird was frequently chief scientist on project cruises. Both were lost at sea off Hawaii in December 1978.

REFERENCES

Arsenev, V. S.
1967 Currents and water masses in the Bering Sea. Transl. 1968, Nat. Mar. Fish. Serv., Northwest Fisheries Center, Seattle.

Barnes, C. A., and T. G. Thompson
1938 Physical and chemical investigations in the Bering Sea and portions of the North Pacific Ocean. Univ. Wash. Pub. in Oceanogr. 3 (2): 33-79.

Brower, W.A. Jr., H.W. Searby, J.L. Wise, H.F. Diaz, and A.S. Prechtel
1977 Climatic atlas of the outer continental shelf waters and coastal regions of Alaska, II, Bering Sea. Arctic Environmental Information and Data Center, Anchorage, Alaska.

Charnell, R. L., and G. A. Krancus
1976 A processing system for Aanderaa current meter data. NOAA Tech. Mem. ERL PMEL-6.

Coachman, L. K., and R. L. Charnell
1979 On lateral water mass interaction—a case study, Bristol Bay, Alaska. J. Phys. Oceanogr. 9: 278-97.

Dodimead, A. J., F. Favorite, and T. Hirano
1963 Salmon of the North Pacific Ocean, II, Review of oceanography of the subarctic Pacific region. Inter. N. Pac. Fish. Comm. Bull. 13.

Favorite, F., A. J. Dodimead, and K. Nasu
1976 Oceanography of the subarctic Pacific region. Inter. N. Pac. Fish. Comm. Bull. 33.

Hebard, J. F.
1961 Currents in the southeastern Bering Sea. Inter. N. Pac. Fish. Comm. Bull. 5: 9-16.

Hughes, F. W., L. K. Coachman, and K. Aagaard
1974 Circulation, transport, and water exchange in the western Bering Sea. *In:* Oceanography of the Bering Sea, D. W. Hood and E. J. Kelley, eds., 59-98. Inst. Mar. Sci., Univ. of Alaska, Occ. Pub. No. 2.

International North Pacific Fisheries Commission
1957 Annual report for the year 1956. INPFC, Vancouver, Canada.

Kinder, T. H.
1977 The hydrographic structure over the continental shelf near Bristol Bay, Alaska. Univ. of Washington, Dep. of Oceanogr. Tech. Rep., Ref.: M77-3.

Kinder, T. H., and L. K. Coachman
1975 An analysis of current meter measurements from Pribilof Canyon. Univ. of Washington Dep. of Oceanogr. Tech. Rep., Ref.: M75-121.

1977 Observation of a bathymetrically trapped current ring. J. Phys. Oceanogr. 7: 946-52.

1978 The front overlaying the continental slope of the eastern Bering Sea. J. Geophys. Res. 83: 4551-9.

Kinder, T. H., L. K. Coachman, and J. A. Galt
1975 The Bering slope current system. J. Phys. Oceanogr. 5: 231-44.

Kinder, T. H., J. D. Schumacher, and D. V. Hansen
1980 Observation of a mesoscale eddy: An example of mesoscale variability in the Bering Sea. J. Phys. Oceanogr. In press.

Kinder, T. H., J. D. Schumacher, R. B. Tripp, and J. C. Haslett
1978 The evolution of the hydrographic structure over the continental shelf near Bristol Bay, Alaska, during summer 1976. Univ. of Washington, Dep. of Oceanogr. Tech. Rep., Ref.: M78-16.

Kitano, K.
1970 A note on the thermal structure of the eastern Bering Sea. J. Geophys. Res. 75: 1110-15.

Kundu, P. J., and J. S. Allen
1976 Some three dimensional characteristics of low frequency current fluctuations near the Oregon coast. J. Phys. Oceanogr. 6: 181-99.

Mayer, D. A., D. V. Hansen, and D. A. Ortman
1979 Long-term current and temperature observations on the middle Atlantic Shelf. J. Geophys. Res. 84: 1776-92.

Muench, R. D., and K. Ahlnäs
1976 Ice movement and distribution in the Bering Sea from March to July, 1974. J. Geophys. Res. 81: 4467-76.

Muench, R. D., and R. L. Charnell
1977 Observations of medium scale features along the seasonal ice edge in the Bering Sea. J. Phys. Oceanogr. 7: 602-6.

Natarov, V. V.
1963 On the water masses and currents of the Bering Sea, Tr. VIRNO, 48; Izv. TINRO. 40 (Transl. 1968: Soviet fisheries investigations in the northeast Pacific, 110-130, NTIS, Springfield, Virginia.)

Naval Oceanographic Office
1977 Surface currents Bering Sea including the Aleutian Islands. Spec. Pub. 1402 NP 5.

Ohtani, K.
1973 Oceanographic structure in the Bering Sea. Memoirs of the Faculty of Fisheries, Hokkaido Univ. 21: 65-106.

Quadfasel, D., and F. Schott
1979 Comparison of different methods of current measurements. Dt. hydrogr. Z. 32: 27-38.

Reed, R. K.
1978 The heat budget of a region in the eastern Bering Sea, summer, 1976. J. Geophys. Res. 83: 3635-45.

Roden, G. I.
1967 On river discharge into the northeastern Pacific Ocean and the Bering Sea. J. Geophys. Res. 72: 5613-29.

Schumacher, J. D., T. H. Kinder, D. J. Pashinski, and R. L. Charnell
1979 A structural front over the continental shelf of the eastern Bering Sea. J. Phys. Oceanogr. 9: 79-87.

Scholl, D. W., E. C. Buffington, and D. M. Hopkins
1968 Geologic history of the continental margin of North America in the Bering Sea. Marine Geol. 6: 297-330.

Straty, R. R.
1977 Current patterns and distributions of river waters in inner Bristol Bay, Alaska. NOAA Tech. Rep. NMFS SSRF-713.

Takenouti, A. Y., and K. Ohtani
1974 Currents and water masses in the Bering Sea: A review of Japanese work. *In:* Oceanography of the Bering Sea, D. W. Hood and E. Kelley, eds., 39-57. Inst. Mar. Sci., Univ. of Alaska, Fairbanks, Occ. Pub. No. 2.

Thompson, W. F., and R. V. Van Cleve
1936 Life history of the Pacific halibut. (2) Distribution and early life history. Rep. Inter. Fish. Comm. 9.

U.S.D.C.
1964 United States coast pilot, Vol. 9, Pacific and Arctic coasts. U.S. Dep. of Commerce, 217.

Wadhams, P.
1978 Wave decay in the marginal ice zone measured from a submarine. Deep Sea Res. 25: 23-40.